Current induced magnetization switching in Co/Cu/Ni-Fe nanopillar with orange peel coupling

D. Aravinthan, P. Sabareesan, and M. Daniel

Current induced magnetization switching in Co/Cu/Ni-Fe nanopillar with orange peel coupling

D. Aravinthan,[1] P. Sabareesan,[2] and M. Daniel[1]

[1]*Centre for Nonlinear Dynamics, School of Physics, Bharathidasan University, Tiruchirappalli - 620 024, India*
[2]*Centre for Nonlinear Science and Engineering, School of Electrical and Electronics Engineering, SASTRA University, Thanjavur - 613 401, India*

The impact of orange peel coupling on spin current induced magnetization switching in a Co/Cu/Ni-Fe nanopillar device is investigated by solving the switching dynamics of magnetization of the free layer governed by the Landau-Lifshitz-Gilbert-Slonczewski (LLGS) equation. The value of the critical current required to initiate the magnetization switching is calculated analytically by solving the LLGS equation and verified the same through numerical analysis. Results of numerical simulation of the LLGS equation using Runge-Kutta fourth order procedure shows that the presence of orange peel coupling between the spacer and the ferromagnetic layers reduces the switching time of the nanopillar device from 67 ps to 48 ps for an applied current density of $4 \times 10^{12} Am^{-2}$. Also, the presence of orange peel coupling reduces the critical current required to initiate switching, and in this case, from $1.65 \times 10^{12} Am^{-2}$ to $1.39 \times 10^{12} Am^{-2}$. © *2015 Author(s). All article content, except where otherwise noted, is licensed under a Creative Commons Attribution 3.0 Unported License.* [http://dx.doi.org/10.1063/1.4927546]

I. INTRODUCTION

Magnetization switching process in nanopillar devices has been a continuously growing topic of research in the recent years, because of its potential applications in ultra-high density recording media,[1] magnetic sensors,[2] magnetic memory devices,[3] read / write heads[3] etc. The nanopillars used for memory devices are in the form of a trilayer consisting of two ferromagnetic layers(pinned layer and free layer) separated by a nonmagnetic spacer. Magnetization switching in this device can be done either by applying a magnetic field or current or both.[4] In this direction, spin polarized current induced magnetization switching has gained considerable interest due to its energy efficiency.[5] The current is applied normal to the plane of the nanopillar. When electrons that constitute the current go through the pinned layer, their spin becomes polarized along the direction of magnetization of the pinned layer. The flow of spin polarized electrons exerts a torque at the interface between spacer layer and the free layer, due to local exchange interaction between conduction electrons and the magnetic moments.[6] The torque applied by non-equilibrium conduction electrons into the free layer is known as spin transfer torque and it is the source for magnetization switching. This concept was first predicted by Slonczewski[7] and later independently by Berger.[8] The spin transfer induced excitations of magnetization were experimentally observed initially in point-contact measurements of Cu/Co multilayers,[6,9] Ni nanowires[10] and later in Co/Cu/Co nanopillar.[11] Since then, spin transfer torque induced switching has been widely studied both theoretically,[12–14] and experimentally[15–17] as well as through numerical and micromagnetic simulations.[18–21] In these studies, the speed of switching of magnetization in magnetic trilayers has been an issue of increasing importance, because of its potential applications. Even though several ways have been put forward to increase the speed of magnetization switching, anisotropy has been found to play a vital role.[22] Among the different anisotropies, magnetic shape anisotropy,[21] magnetocrystalline anisotropy[23] and surface anisotropy[24] reduce the switching time drastically.

5, 077166-1

It is very difficult to grow multilayer nanopillars in an ideal layer by layer fashion. The resultant multilayers have certain interface roughness or even discontinuities, and they give rise to different coupling mechanisms. The first among them is the pinhole coupling, which arises due to discontinuities in the nonmagnetic layer.[25] The second one is the Ruderman-Kittel-Kasuya-Yosida (RKKY) interaction which arises due to the oscillation of electrons, in the Fermi surface of the spacer material.[26] There are two more coupling mechanisms, which arises due to the roughness of the layers.[27] The first one is the biquadratic coupling which occurs when the roughness of the free and pinned layers are uncorrelated.[28] The next one is the orange peel coupling or Néel coupling, which results from the dipole interaction between two ferromagnetic layers separated by a nonmagnetic spacer layer with correlated interface roughness.[29] When the thickness of the spacer layer is of the order of few nanometres, the orange peel coupling dominates.[30] When the nonmagnetic spacer layer has the correlated waviness interface, and the magnetization of the two ferromagnetic layers are parallel to each other, magnetostatic charges of opposite sign appear symmetrically on the opposing interfaces. The dipole interaction between these opposing charges gives rise to a ferromagnetic coupling between the magnetization of the two ferromagnetic layers known as orange peel coupling[31] referred so because of the dimpled texture of an orange[32] and produce a coupling field normal to the magnetization of the easy axis. Hence, it is expected to contribute to the reduction in switching time. Although the biquadratic coupling favors the perpendicular alignment of the free and pinned layers magnetization, this effect is not considered in this paper. The concept of orange peel coupling was originally developed for thick layer systems and later it was extended to nanopillar multilayer systems by Kools et al.[33] In their paper, Kools et al studied about the effect of finite magnetic film thickness on Néel coupling in spinvalves by taking different types of roughness in the nanopillar structure. Schrag et al[34] studied about the Néel orange peel coupling in magnetic tunnel junctions and showed that Néel field (orange peel coupling field) depends on barrier layer thickness. Schulthess and Butler[35] investigated the Néel coupling due to correlated roughness in spinvalves both analytically and numerically and showed that Néel's field is inversely proportional to the spacer layer thickness. The nature of magnetization reversal is experimentally observed by the measurement of **M**-**H** loops, and showed that the coercivity enhancement in the free layer results from the orange peel coupling.[36] Kim et al[37] experimentally found that the orange peel coupling field increases with the decrease in the free layer thickness. Moritz et al[38] both theoretically and experimentally showed that the orange peel coupling favours the parallel magnetic alignment of the magnetization in the ferromagnetic layers. However, there is a lack of understanding about the effect of orange peel coupling on the spin current induced magnetization switching in nanopillars. Therefore, in the present paper, we investigate the impact of orange peel coupling on spin current induced magnetization switching in a Co/Cu/Ni-Fe nanopillar theoretically. This is carried out by solving the magnetization switching dynamics of the free ferromagnetic layer governed by the Landau-Lifshitz-Gilbert-Slonczewski (LLGS) equation both analytically and numerically.

The paper is structured as follows. In Section II, the geometry of the Co/Cu/Ni-Fe nanopillar device is described and the dynamics expressed in-terms of the LLGS equation. The expression for critical current density and its value required to initiate switching of the free layer magnetization is calculated in Section III. Section IV is devoted to numerical simulation of the LLGS equation, to find the impact of orange peel coupling, the current density and the thicknesses of the spacer as well as the free layer on the switching time. The results are concluded in Section V.

II. MAGNETIZATION SWITCHING DYNAMICS IN TRILAYER NANOPILLAR

The trilayer nanopillar considered for our study in this paper consists of two ferromagnetic layers (Co, Ni-Fe) sandwiched by a nonmagnetic (Cu) spacer layer. A schematic sketch of the above device is shown in FIG. 1. The ferromagnetic Cobalt layer with a thickness of 4 nm possessing high coercivity, whose magnetization($\mathbf{M}_p$) is fixed and lies parallel to the plane of the layer and along x-direction forms the pinned layer. The single domain ferromagnetic free layer with thickness same as pinned layer (4 nm) is made up of the low coercivity material Permalloy (Ni-Fe) with an in-plane magnetization ($\mathbf{M}$) which is free to move. The middle spacer layer is made up of the nonmagnetic metal Copper (Cu) and its thickness(2 nm) is small enough to transfer the polarized
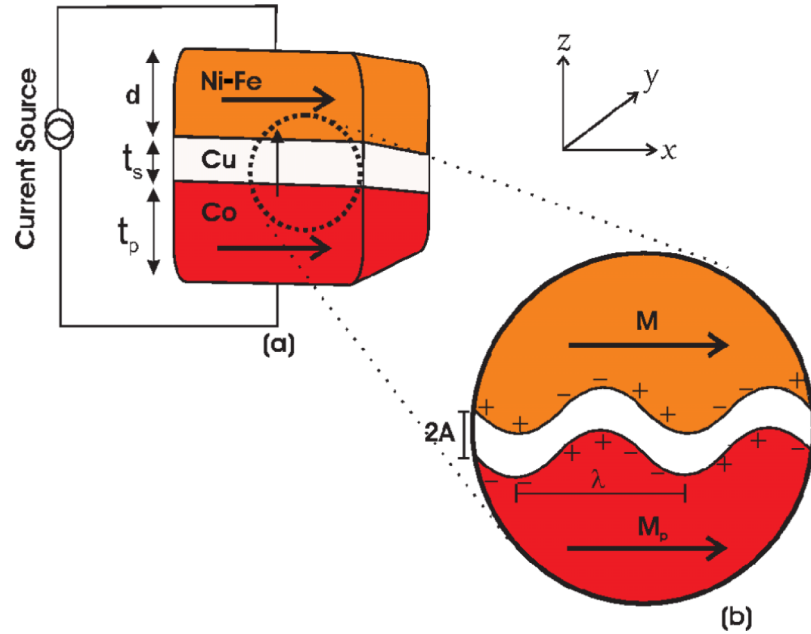
FIG. 1. (a). A sketch of the Co/Cu/Ni-Fe nanopillar device. Co is the pinned layer and Ni-Fe is the free layer. Cu represents the nonmagnetic spacer layer. d, t_s and t_p are the thickness of the free layer, spacer layer and pinned layer respectively. (b). In the zoomed view, we see the nonmagnetic spacer layer interface has the correlated waviness with wavelength λ and amplitude A. **M** and $\mathbf{M}_p$ represent the magnetization of the free layer and pinned layer respectively. When the magnetization of two ferromagnetic layers are parallel, magnetostatic charges(-,+) of opposite sign(+,-) appear symmetrically on opposing interfaces.

current from the Co - pinned layer to the Ni-Fe - free layer. If the thickness of the spacer layer is high, the orange peel coupling between the ferromagnetic layers does not occur. Current is applied along z-direction of the nanopillar device, which is normal to the plane of the nanopillar and it becomes spin polarized while passing through the Cobalt layer. When the spin polarized current reaches the Permalloy layer via the Copper, it produces a torque due to the change in the spin angular momentum.[39] This spin transfer torque switches the magnetization of the free layer. The Landau-Lifshitz-Gilbert-Slonczewski(LLGS) equation[40] that governs the switching dynamics of magnetization of the free layer is written as

$$\frac{1}{\gamma}\frac{d\mathbf{M}}{dt} = -[\mathbf{M} \times \mathbf{H}_{eff}] - \frac{\alpha}{M_s}[\mathbf{M} \times (\mathbf{M} \times \mathbf{H}_{eff})] + a_j[\mathbf{M} \times (\mathbf{M} \times \mathbf{M}_p)]. \tag{1a}$$

$$\mathbf{M} = (M^x, M^y, M^z), \qquad \mathbf{M}^2 = M^{x^2} + M^{y^2} + M^{z^2} = M_s^2. \tag{1b}$$

Here, $\mathbf{M} = (M^x, M^y, M^z)$ is the magnetization and M_s is the saturation magnetization of the Ni-Fe - free layer. The unit magnetization vector $\mathbf{M}_p$ represents the magnetization of the pinned layer. γ is the gyromagnetic ratio of the free electron, α is the Gilbert damping parameter, and $a_j = \frac{pJ\hbar}{\mu_0 edM_s^2}$ is the spin transfer torque coefficient. The current flows from the pinned layer to the free layer, and so positive value is assigned to the spin transfer coefficient a_j in Eq. (1). p is the polarization factor, J is the current density applied from the source, $\hbar$ is the reduced Planck's constant, μ_0 is the permeability of free space, e is the electron's charge and d is the thickness of the free layer.

In the LLGS equation (1a), the first term in the right hand side describes the precession of magnetization which conserves the magnetic energy and it determines the precessional frequency of the magnetization dynamics. The second term represents the Gilbert damping which dissipates energy during the dynamics. The spin transfer term proportional to a_j either amplifies or attenuates the precessional motion, depending on the direction of the current flow. The effective field $\mathbf{H}_{eff}$ due to various magnetic contributions acting on the free layer contains the following components.

$$\mathbf{H}_{eff} = \mathbf{H}_{ma} + \mathbf{H}_{shape} + \mathbf{H}_{ext} + \mathbf{H}_{opc}. \tag{2}$$

As the permalloy free layer of the nanopillar device has in-plane magnetocrystalline anisotropy along its easy axis(x-direction), the corresponding field is written as

$$\mathbf{H}_{ma} = h_a M^x \mathbf{e}^x, \tag{3}$$

where $\mathbf{e}^x$ is the unit vector along x-direction and $h_a = \frac{2k_a}{\mu_0 M_s^2}$. Here k_a is the magnetocrystalline anisotropy coefficient. Nonspherical sample always has a shape anisotropy caused by a demagnetizing field. Having chosen a nanofilm as the free layer of the nanopillar, the shape anisotropy plays a major role in magnetization switching here. The effective field contribution due to shape anisotropy can be written as

$$\mathbf{H}_{shape} = -[N_x M^x \mathbf{e}^x + N_y M^y \mathbf{e}^y + N_z M^z \mathbf{e}^z], \tag{4}$$

where N_x, N_y, N_z are the demagnetization factors, and $\mathbf{e}^x, \mathbf{e}^y, \mathbf{e}^z$ represent the unit vectors along x, y and z directions respectively. The value of the demagnetization factors depends upon the shape of the material. Since, our free layer lies in the xy-plane, the values of the demagnetization factors are given by $N_x = N_y = 0$ and $N_z = 1$. Hence, the field due to shape anisotropy can be written as

$$\mathbf{H}_{shape} = -N_z M^z \mathbf{e}^z. \tag{5}$$

When an external magnetic field H_e is applied normal to the easy axis of magnetization, that is along y-direction, the contributory field is written as

$$\mathbf{H}_{ext} = H_e \mathbf{e}^y. \tag{6}$$

Since the free and pinned layers magnetization are initially assumed to be in-plane and the magnetizations are perpendicular to the roughness i.e. along the easy axis, the ferromagnetic coupling occur perpendicular to the easy axis[30] and the coupling field strength can be written as,

$$\mathbf{H}_{opc} = h_n M^y \mathbf{e}^y, \tag{7}$$

where $h_n = \frac{\pi^2 h^2}{\sqrt{2}\lambda d} \exp\left(\frac{-2\sqrt{2}\pi t_s}{\lambda}\right)$, h_n is the magnitude of the coupling field strength called as Néel field.[34,41] The field $\mathbf{H}_{opc}$ is acting normal to the easy axis of magnetization in the plane, that is along y-direction. Hence, the total effective field acting on the free layer can be written using Eqs. (2)-(7) as

$$\mathbf{H}_{eff} = h_a M^x \mathbf{e}^x - N_z M^z \mathbf{e}^z + H_e \mathbf{e}^y + h_n M^y \mathbf{e}^y. \tag{8}$$

The total effective field can be written in the dimensionless form by taking $\mathbf{M} = M_s\mathbf{m}$, $\mathbf{H}_e = M_s\mathbf{h}_e$ and $\mathbf{H}_{eff} = M_s\mathbf{h}_{eff}$ as,

$$\mathbf{h}_{eff} = h_a m^x \mathbf{e}^x + (h_e + h_n m^y)\mathbf{e}^y - N_z m^z \mathbf{e}^z. \tag{9}$$

By substituting the effective field found in Eq. (9) in Eq. (1), we obtain the dynamical equation(LLGS equation) as

$$\frac{d\mathbf{m}}{d\tau} = -[\mathbf{m} \times (h_a m^x \mathbf{e}^x + (h_e + h_n m^y)\mathbf{e}^y - N_z m^z \mathbf{e}^z)] \tag{10a}$$

$$-\alpha[\mathbf{m} \times (\mathbf{m} \times (h_a m^x \mathbf{e}^x + (h_e + h_n m^y)\mathbf{e}^y - N_z m^z \mathbf{e}^z))] + a_j[\mathbf{m} \times (\mathbf{m} \times \mathbf{m}_p)].$$

$$\mathbf{m} = (m^x, m^y, m^z), \qquad \mathbf{m}^2 = m^{x2} + m^{y2} + m^{z2} = 1. \tag{10b}$$

Eq. (10) is the dimensionless form of the LLGS equation which is obtained by using the dimensionless variables $\mathbf{m}$, $\mathbf{m}_p$, $\mathbf{h}_{eff}$ and dimensionless time $\tau = \gamma M_s t$. The magnetization switching dynamics of the nanopillar device can be understood by solving Eq. (10). Before actually solving Eq. (10), first we calculate the critical current required for switching the magnetization of the free layer.

III. CRITICAL CURRENT DENSITY FOR MAGNETIZATION SWITCHING

The spin transfer torque will switch the magnetization of the free layer and it can occur only above a critical value of the applied current.[18] The critical value of the current density can be

calculated analytically from the time independent solution of the LLGS equation(Eq. (10)). In the static limit ($\frac{dm}{dt} = 0$), the damping term($\mathbf{M} \times \frac{d\mathbf{M}}{dt}$) vanishes. To obtain the stationary solution of the LLGS equation, we write the LLGS equation(10a) in the component form for the static case as,

$$(N_z + h_n)m^y m^z + h_e m^z - a_j((m^y)^2 + (m^z)^2) = 0, \tag{11}$$

$$-(h_a + N_z)m^x m^z + a_j m^x m^y = 0, \tag{12}$$

$$(h_a - h_n)m^x m^y - h_e m^x + a_j m^x m^z = 0. \tag{13}$$

Solving Eqs. (12) and (13) algebraically, the time independent solution for m^z is obtained as

$$m^z = \frac{h_e a_j}{a_j^2 + [(h_a - h_n)(h_a + N_z)]}. \tag{14}$$

The stationary solution of m^y can be obtained by substituting the value of m^z found in Eq. (14) into Eq. (12) as

$$m^y = \frac{h_e(h_a + N_z)}{a_j^2 + [(h_a - h_n)(h_a + N_z)]}. \tag{15}$$

The time independent solution of m^x is obtained by substituting the values of m^y and m^z in the length constraint equation (Eq. (10b)). The resultant solution reads

$$m^x = \left[1 - \frac{h_e^2[(h_a + N_z)^2 + a_j^2]}{[a_j^2 + (h_a - h_n)(h_a + N_z)]^2} \right]^{\frac{1}{2}}. \tag{16}$$

It can be verified that Eq. (11) satisfies identically for the values of m^x, m^y, and m^z found in Eqs. (14)-(16). The critical current density for magnetization switching is obtained by using the time independent solutions given in Eqs. (14)-(16) as initial conditions. The free layer magnetization is initially aligned along the easy axis, i.e. along x-direction, so that the initial conditions are $m^x = 1$, $m^y = 0$ and $m^z = 0$. If the free layer magnetization satisfies the above initial conditions, then the magnetization switching can occur when the value of m^x becomes zero.[4] i.e. when,

$$h_e^2[(h_a + N_z)^2 + a_j^2] = [a_j^2 + (h_a - h_n)(h_a + N_z)]^2. \tag{17}$$

As the magnetic layers of our device lie in the xy-plane, the demagnetizing field due to shape anisotropy guarantees the pinned layer magnetization to lie always along the positive x-direction. Hence, there is no need to apply any external field to retain its magnetization. Using the above condition (Eq. (17)) and switching off the external applied field ($h_e = 0$), we get a_j^2 as,

$$a_j^2 = (h_n - h_a)(h_a + N_z). \tag{18}$$

By substituting the value of a_j ($a_j = \frac{pJ\hbar}{\mu_0 edM_s^2}$) into Eq. (18), the expression for the critical current density J_c is obtained as

$$J_c = \left(\frac{\mu_0 edM_s^2}{p\hbar} \right) [(h_n - h_a)(h_a + N_z)]^{\frac{1}{2}}. \tag{19}$$

The above expression shows that the critical or the threshold current density depends on the thickness of the free layer(d), magnetocrystalline anisotropy(h_a), shape anisotropy(N_z) and the orange peel coupling(h_n). The critical current density takes non-zero value and magnetization switching occurs only when the orange peel coupling field is greater than the magnetocrystalline anisotropy. The switching occurs even in the case of isotropic free layer (i.e. $h_a = 0$). This is because the orange peel coupling generates a field normal to the easy axis, which forces the free layer magnetization to go out of the plane. The actual value of the threshold or critical current density required to initiate the switching of the magnetization of the permalloy free layer is calculated from Eq. (19) by substituting the values of all the respective experimental parameters found in TABLE I. The resultant value of the critical current density in the presence of the orange peel coupling reads

TABLE I. Experimental values of various parameters of Permalloy(Ni-Fe) material[43] and constants[4] used in the calculations.

Parameter / Constant	Symbol	Value
Charge of an electron	e	$1.602 \times 10^{-19} C$
Reduced Planck's constant	$\hbar$	$1.0551 \times 10^{-34} Js$
Gyromagnetic ratio of free electron	γ	$2.21 \times 10^5 m A^{-1} s^{-1}$
Permeability of free space	μ_0	$1.257 \times 10^{-6} J A^{-2} m^{-1}$
Polarization factor	p	0.4
Gilbert damping parameter	α	0.001
Magnetocrystalline anisotropy coefficient of Ni-Fe	k_a	$2 \times 10^3 J m^{-3}$
Saturation magnetization of Ni-Fe	M_s	$0.795 \times 10^6 A m^{-1}$
Thickness of the free layer (Ni-Fe)	d	$4 \times 10^{-9} m$
Thickness of the spacer layer (Cu)	t_s	$2 \times 10^{-9} m$
Amplitude of the interface waviness	A	$0.8 \times 10^{-9} m$
Wavelength of the interface waviness	λ	$40 \times 10^{-9} m$

$1.37 \times 10^{12} Am^{-2}$ and in the absence of orange peel coupling reads $1.70 \times 10^{12} Am^{-2}$. The calculated critical current density in the absence of orange peel coupling is consistent with the already available micromagnetic simulation[20,42] results which lie between $0.5 \times 10^{12} Am^{-2}$ and $3.0 \times 10^{12} Am^{-2}$. As the magnetization switching dynamics of the permalloy free layer is governed by the LLGS equation, which is a highly non-trivial vector nonlinear differential equation, it cannot be solved analytically in the more general case. Therefore, in the forthcoming section, the magnetization switching dynamics of the free layer is understood by numerically solving the LLGS Equation(10a).

IV. MAGNETIZATION SWITCHING: A NUMERICAL STUDY

The magnetization switching dynamics governed by the LLGS equation(Eq. (10a)) is numerically integrated using fourth order Runge-Kutta(RK4) procedure for different cases. First, the response of magnetization of the free layer **M** to the current is studied by varying the applied current density. Then, to find the impact of orange peel coupling on magnetization switching time, the LLGS equation is computed both in the presence and in the absence of orange peel coupling separately. Finally, the impact of the thicknesses of the spacer layer and the free layer on switching time is investigated by varying the thickness of the spacer layer and the free layer. Since we study the impact of current induced magnetization switching only, the magnetic field is switched off ($h_e = 0$). The value of the Gilbert damping parameter is chosen as, $\alpha = 0.001$ to suppress the ringing effect. After solving the dimensionless LLGS equation (Eq. (10a)), the dimensionless time variable τ is converted into dimension t by using the transformation $t = \tau/\gamma M_s$. Unless specified otherwise, the values of the various material parameters and constants given in TABLE I are used throughout the paper.

A. Impact of current density on switching time

In the previous section, we analytically found that, with orange peel coupling, magnetization switching occurs only above the critical value of current density, namely $1.37 \times 10^{12} Am^{-2}$. To confirm this, and to study the impact of current density on the switching time, the LLGS Equation(10a) is numerically solved both in the presence and in the absence of orange peel coupling by varying the current density upto $10 \times 10^{12} Am^{-2}$. The data obtained from numerical simulation is plotted in FIG. 2, which confirms that the magnetization switching occurs only above the critical current density and its value in the presence of orange peel coupling is $1.39 \times 10^{12} Am^{-2}$, which is very close to the analytical result obtained($1.37 \times 10^{12} Am^{-2}$). The value of the critical current density without orange peel coupling is found as $1.65 \times 10^{12} Am^{-2}$ (see FIG. 2) and the corresponding value through analytical study is $1.70 \times 10^{12} Am^{-2}$. Thus, the critical current density required to initiate switching reduces from $1.65 \times 10^{12} Am^{-2}$ to $1.39 \times 10^{12} Am^{-2}$ when there exists orange peel coupling. The reason behind this is that, orange peel coupling utilizes the interface waviness of
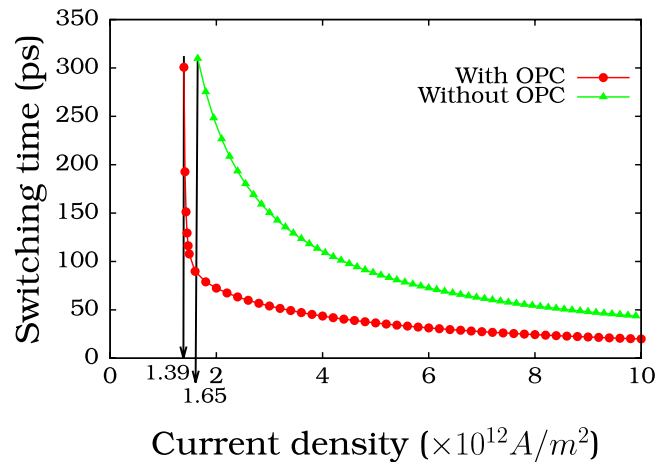
FIG. 2. A plot of current density versus switching time in the presence and in the absence of the orange peel coupling(OPC). From the plot, the value of critical current density is $J_c = 1.39 \times 10^{12} Am^{-2}$ in the presence of orange peel coupling and $J_c = 1.65 \times 10^{12} Am^{-2}$ when their is no orange peel coupling.

correlated layers and produces a field normal to the easy axis of magnetization. This additional field acts on the free layer magnetization along with spin polarized current and pulls it out of the plane. Hence, the critical current density required to switch the free layer magnetization is reduced.

The effect of current density on the switching time can be understood through the plots in FIG. 3. In FIG. 3, we have plotted the switching time against magnetization of the free layer for different values of current density. From the plots, it is observed that, when the current density is increased from $2 \times 10^{12} Am^{-2}$ to $10 \times 10^{12} Am^{-2}$, the switching time decreases from 78 ps to 23 ps. When the applied current density is high, the transfer of angular momentum from the electrons of the spin polarized current to the free layer is high and the value of spin transfer torque exerted on the free layer is large, and therefore the switching time is reduced. When the applied current is increased further, the switching time approaches a small value asymptotically. Hence, increasing the applied current density above $10 \times 10^{12} Am^{-2}$ is not salient for reducing the switching time. As one can see from FIG. 3, switching time of permalloy free layer is of the order of few picoseconds, which is in good agreement with the results of the micromagnetic simulation[42] and experiment.[44]

B. Impact of orange peel coupling on switching time

For the Co/Cu/Ni-Fe nanopillar, the magnetization of the free layer against the switching time in the presence and absence of orange peel coupling is plotted using the results of our numerical
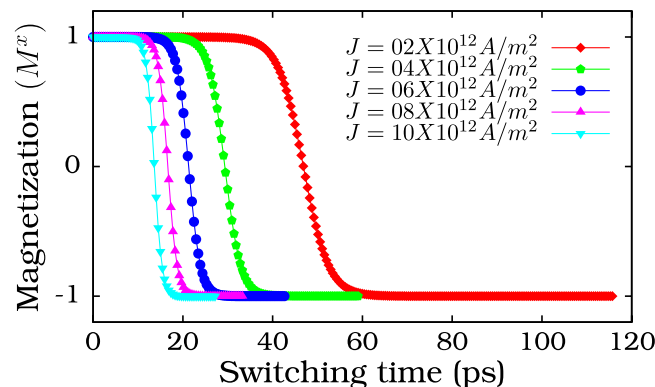

FIG. 3. A plot of free layer magnetization versus switching time for the Co/Cu/Ni-Fe nanopillar for different current density. The applied current density is increased from $2 \times 10^{12} Am^{-2}$ to $10 \times 10^{12} Am^{-2}$. The switching time decreases from 78 ps to 23 ps.
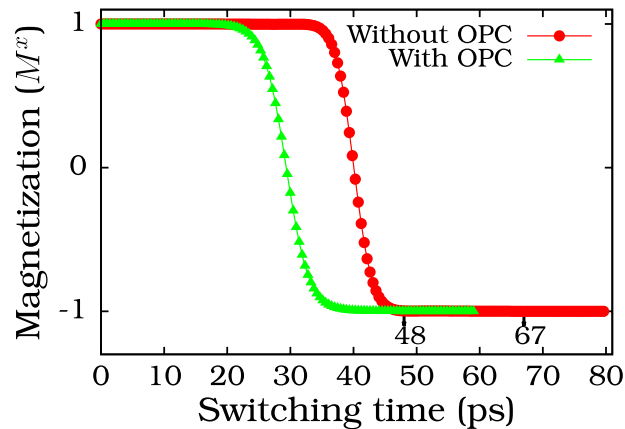
FIG. 4. A plot of free layer magnetization versus switching time for the Co/Cu/Ni-Fe nanopillar in the presence and absence of the orange peel coupling for an applied current density of $J = 4 \times 10^{12} Am^{-2}$. The presence of orange peel coupling reduces the switching time from 67 ps to 48 ps.

study in FIG. 4, for an applied current density of $J = 4 \times 10^{12} Am^{-2}$. Initially, the free layer magnetization is aligned along the positive x-direction ($\mathbf{M}$=(1,0,0)). The applied current switches the magnetization from the initial stable state of ($\mathbf{M}$=(1,0,0)) to another stable state ($\mathbf{M}$=(-1,0,0)) by coherent rotation of the magnetization. In the absence of orange peel coupling, the switching time, i.e. the time required to switch the magnetization from the state ($\mathbf{M}$=(1,0,0)) to the state ($\mathbf{M}$=(-1,0,0)) is 67 ps. It is found that, the presence of orange peel coupling reduces the switching time from 67 ps to 48 ps. The field produced by the orange peel coupling added with the spin transfer torque, moves the magnetization of the free layer from in-plane to out of plane very fast. This generates a demagnetizing field normal to the film plane which forces the free layer magnetization into the plane(reversed state). Thus, the field due to orange peel coupling combined with the demagnetizing field due to shape anisotropy reduce the switching time drastically. Since, orange peel coupling depends on the thickness of the spacer layer and free layer, their individual effect on reducing the switching time is discussed in the forthcoming sections.

C. Impact of spacer layer thickness on switching time

In order to understand the impact of impact of spacer layer thickness on the switching time, we vary the spacer layer thickness from 1 nm to 10 nm for an applied current density of $J = 4 \times 10^{12} Am^{-2}$ while solving the LLGS equation (Eq. (10a)) numerically and the resultant data are plotted in FIG. 5. From the figure it is observe that with increase in the spacer layer thickness, the field due to orange peel coupling decreases exponentially and therefore, the time required to move the free layer magnetization from in-plane to out of plane increases. Thus, switching time increases with an increase in the thickness of the spacer layer. However, when the thickness of the spacer layer increases beyond 10 nm, there is a subtle change in the switching time. This is because at this point, the effect of orange peel coupling vanishes and the switching occurs only due to the spin transfer torque effect. Thus, the switching time can be reduced by constructing the trilayer nanopillar using a spacer layer with minimum thickness and with orange peel coupling. For instance, for a thickness of 2 nm of the spacer layer, in the presence of orange peel coupling, the switching time is calculated from FIG. 5 as 48 ps, which agrees perfectly with the result in FIG. 4.

D. Impact of free layer thickness on switching time

As the free layer thickness plays a key role in the reduction of switching time, its impact on the switching time is studied by solving the LLGS equation (Eq. (10a)) with an applied current density of $J = 4 \times 10^{12} Am^{-2}$. The thickness of the free layer is varied from 1 nm to 10 nm and the
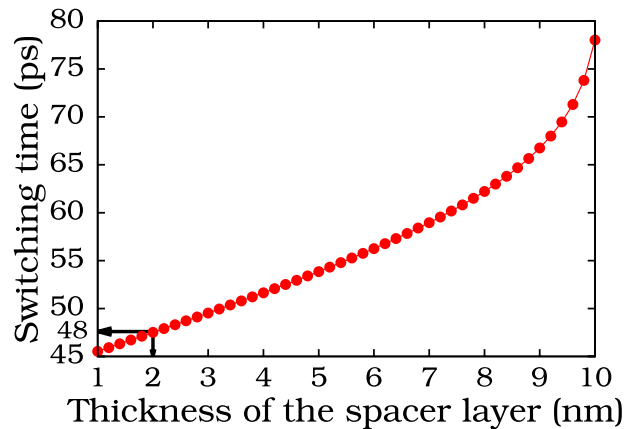
FIG. 5. A plot of the thickness of the spacer layer versus switching time for the Co/Cu/Ni-Fe nanopillar for an applied current density $J = 4 \times 10^{12} Am^{-2}$. Switching time increases when the thickness of the spacer layer increases.
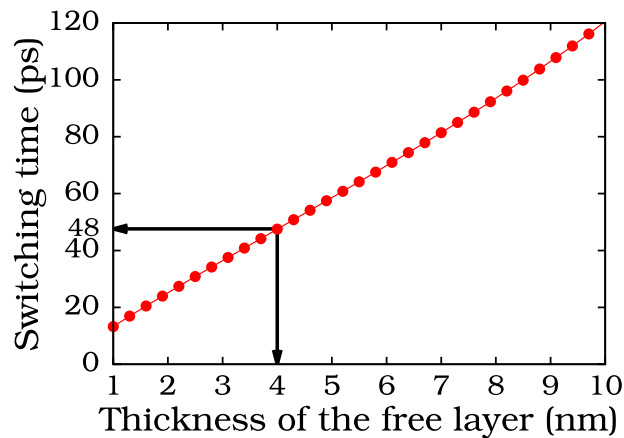
FIG. 6. A plot of the thickness of the free layer versus switching time for the Co/Cu/Ni-Fe nanopillar for an applied current density of $J = 4 \times 10^{12} Am^{-2}$. Switching time decreases when the thickness of the free layer is reduced.

data obtained from numerical simulation is plotted in FIG. 6. The switching time reduces when the thickness of the free layer is decreased. The reason behind this is that the field due to orange peel coupling and spin-transfer torque increase when the free layer thickness decreases. For large orange peel coupling and spin-transfer torque, the time taken for the free layer magnetization to go from in-plane to out of plane reduces drastically. Hence, fast switching can be achieved by making the free layer of the nanopillar device with minimal thickness in the presence of orange peel coupling. From FIG. 6, the switching time, in the case of a free layer with thickness 4 nm in the presence of orange peel coupling is calculated as 48 ps and it coincides well with the value for the same in FIG. 4.

V. CONCLUSIONS

In this paper, spin current induced magnetization switching in Co/Cu/Ni-Fe nanopillar device with orange peel coupling is investigated. The switching dynamics of magnetization of the permalloy(Ni-Fe) free layer is studied by solving the governing LLGS equation. The LLGS equation is solved analytically in the static case and the critical or threshold current density is found out. The value of critical current density required to initiate the magnetization switching for our device, in the presence of orange peel coupling is obtained as $1.39 \times 10^{12} Am^{-2}$ and in the absence of orange

peel coupling, its value is found as $1.65 \times 10^{12} Am^{-2}$. The more general LLGS equation is numerically integrated using Runge-Kutta fourth order procedure. The results show that, in the absence of orange peel coupling, the switching time is 67 ps and it reduces to 48 ps when there exists an orange peel coupling between the ferromagnetic layers. Since, orange peel coupling depends on the thickness of the spacer layer and free layer, their individual effect on the switching time has been studied here. The switching time increases from 45 ps to 78 ps, when the thickness of the spacer layer is increased from 1 nm to 10 nm. Similarly, when the thickness of the free layer is increased from 1 nm to 10 nm, the switching time increases from 14 ps to 115 ps.

In conclusion, the critical current density depends on the thickness of the free layer, magnetocrystalline anisotropy, shape anisotropy and orange peel coupling. The presence of orange peel coupling between the ferromagnetic layers reduces the critical current density required to initiate switching, and the switching time by quickly moving the free layer magnetization from in-plane to out of plane. Fast magnetization switching can be achieved by making the free layer and a spacer layer of the nanopillar device, with minimal thicknesses in the presence of orange peel coupling.

ACKNOWLEDGEMENTS

[1] S. Krause, L. Berbil-Bautista, G. Herzog, M. Bode, and R. Wiesendanger, Science **317**, 1537 (2007).
[2] S. Wolf, D. Awschalom, R. Buhrman, J. Daughton, S. Von Molnar, M. Roukes, A. Y. Chtchelkanova, and D. Treger, Science **294**, 1488 (2001).
[3] C. Chappert, A. Fert, and F. N. Van Dau, Nat. Mater. **6**, 813 (2007).
[4] P. Sabareesan and M. Daniel, Phys. Scr. **84**, 035706 (2011).
[5] J. Sun, Nature **425**, 359 (2003).
[6] E. Myers, D. Ralph, J. Katine, R. Louie, and R. Buhrman, Science **285**, 867 (1999).
[7] J. C. Slonczewski, J. Magn. Magn. Mater. **159**, L1 (1996).
[8] L. Berger, Phys. Rev. B **54**, 9353 (1996).
[9] M. Tsoi, A. Jansen, J. Bass, W.-C. Chiang, M. Seck, V. Tsoi, and P. Wyder, Phys. Rev. Lett. **80**, 4281 (1998).
[10] J.-E. Wegrowe, D. Kelly, Y. Jaccard, P. Guittienne, and J.-P. Ansermet, Europhys. Lett. **45**, 626 (1999).
[11] J. Katine, F. Albert, R. Buhrman, E. Myers, and D. Ralph, Phys. Rev. Lett. **84**, 3149 (2000).
[12] X. Waintal, E. B. Myers, P. W. Brouwer, and D. C. Ralph, Phys. Rev. B **62**, 12317 (2000).
[13] S. Zhang, P. M. Levy, and A. Fert, Phys. Rev. Lett. **88**, 236601 (2002).
[14] M. Stiles and A. Zangwill, J. Appl. Phys. **91**, 6812 (2002).
[15] J. Grollier, V. Cros, A. Hamzic, J.-M. George, H. Jaffres, A. Fert, G. Faini, J. Ben Youssef, and H. Legall, Appl. Phys. Lett. **78**, 3663 (2001).
[16] S. I. Kiselev, J. Sankey, I. Krivorotov, N. Emley, R. Schoelkopf, R. Buhrman, and D. Ralph, Nature **425**, 380 (2003).
[17] B. Özyilmaz, A. D. Kent, J. Z. Sun, M. J. Rooks, and R. H. Koch, Phys. Rev. Lett. **93**, 176604 (2004).
[18] Z. Li and S. Zhang, Phys. Rev. B **68**, 024404 (2003).
[19] J. Xiao, A. Zangwill, and M. D. Stiles, Phys. Rev. B **72**, 014446 (2005).
[20] E. Martinez, L. Torres, L. Lopez-Diaz, M. Carpentieri, and G. Finocchio, J. Appl. Phys. **97**, 10E302 (2005).
[21] Z. Xiao, X. Ma, P. Wu, J. Zhang, L. Chen, and S. Shi, J. Appl. Phys. **102**, 093907 (2007).
[22] S. Mangin, D. Ravelosona, J. Katine, M. Carey, B. Terris, and E. E. Fullerton, Nat. Mater. **5**, 210 (2006).
[23] A. Kent, B. Özyilmaz, and E. Del Barco, Appl. Phys. Lett. **84**, 3897 (2004).
[24] M. Daniel and P. Sabareesan, J. Magn. Magn. Mater. **322**, 675 (2010).
[25] P. Grünberg, R. Schreiber, Y. Pang, M. Brodsky, and H. Sowers, Phys. Rev. Lett. **57**, 2442 (1986).
[26] M. A. Ruderman and C. Kittel, Phys. Rev. **96**, 99 (1954); T. Kasuya, Prog. Theor. Phys. **16**, 45 (1956); K. Yosida, Phys. Rev. **106**, 893 (1957); P. Bruno and C. Chappert, Phys. Rev. Lett. **67**, 1602 (1991).
[27] M. Stiles, in *Ultrathin Magnetic Structures III*, edited by J. Bland and B. Heinrich (Springer, Berlin Heidelberg, 2005) pp. 99–142.
[28] S. Demokritov, E. Tsymbal, P. Grünberg, W. Zinn, and I. K. Schuller, Phys. Rev. B **49**, 720 (1994).
[29] L. Néel, C. R. Acad. Sci., **255**, 1676 (1962).
[30] Y. Pennec, J. Camarero, J. C. Toussaint, S. Pizzini, M. Bonfim, F. Petroff, W. Kuch, F. Offi, K. Fukumoto, F. Nguyen Van Dau, and J. Vogel, Phys. Rev. B **69**, 180404 (2004).
[31] B. Diény, in *Magnetism*, edited by É. du Trémolet de Lacheisserie, D. Gignoux, and M. Schlenker (Springer, New York, 2005) pp. 255–304.
[32] S. Russek, R. McMichael, M. Donahue, and S. Kaka, in *Spin Dynamics in Confined Magnetic Structures II*, edited by B. Hillebrands and K. Ounadjela (Springer, Berlin Heidelberg, 2003) pp. 93–156.
[33] J. Kools, W. Kula, D. Mauri, and T. Lin, J. Appl. Phys. **85**, 4466 (1999).
[34] B. Schrag, A. Anguelouch, S. Ingvarsson, G. Xiao, Y. Lu, P. Trouilloud, A. Gupta, R. Wanner, W. Gallagher, P. Rice, and S. Parkin, Appl. Phys. Lett. **77**, 2373 (2000).
[35] T. Schulthess and W. Butler, J. Appl. Phys. **87**, 5759 (2000).

[36] H. D. Chopra, D. X. Yang, P. J. Chen, D. C. Parks, and W. F. Egelhoff, Phys. Rev. B **61**, 9642 (2000).

[37] K. Kim, S. Jang, K. Shin, H. Kim, and T. Kang, J. Appl. Phys. **89**, 7612 (2001).

[38] J. Moritz, F. Garcia, J. Toussaint, B. Dieny, and J. Nozieres, Europhys. Lett. **65**, 123 (2004).

[39] Y. B. Bazaliy, B. Jones, and S.-C. Zhang, J. Appl. Phys. **89**, 6793 (2001).

[40] T. Devolder, H. Schumacher, and C. Chappert, in *Spin Dynamics in Confined Magnetic Structures III*, edited by B. Hillebrands and A. Thiaville (Springer, Berlin Heidelberg, 2006) pp. 1–55.

[41] A. Anguelouch, B. Schrag, G. Xiao, Y. Lu, P. Trouilloud, R. Wanner, W. Gallagher, and S. Parkin, Appl. Phys. Lett. **76**, 622 (2000).

[42] B. Choi, J. Rudge, E. Girgis, J. Kolthammer, Y. Hong, and A. Lyle, Appl. Phys. Lett. **91**, 022501 (2007).

[43] J. Zhang and R. White, IEEE Trans. Magn. **32**, 4630 (1996).

[44] N. C. Emley, I. N. Krivorotov, O. Ozatay, A. G. F. Garcia, J. C. Sankey, D. C. Ralph, and R. A. Buhrman, Phys. Rev. Lett. **96**, 247204 (2006).